Cell Stem Cell
Short Article

Muscle Satellite Cells Are Primed for Myogenesis but Maintain Quiescence with Sequestration of *Myf5* mRNA Targeted by microRNA-31 in mRNP Granules

Colin G. Crist,[1,2] Didier Montarras,[1] and Margaret Buckingham[1,*]
[1]CNRS URA 2578, Department of Developmental Biology, Institut Pasteur, 25 Rue du Dr. Roux, 75724 Paris Cedex 15, France
[2]Present address: Lady Davis Institute for Medical Research and Department of Human Genetics, McGill University, Montreal, QC H3A 1B1, Canada
*Correspondence: margaret.buckingham@pasteur.fr
http://dx.doi.org/10.1016/j.stem.2012.03.011

SUMMARY

Regeneration of adult tissues depends on stem cells that are primed to enter a differentiation program, while remaining quiescent. How these two characteristics can be reconciled is exemplified by skeletal muscle in which the majority of quiescent satellite cells transcribe the myogenic determination gene *Myf5*, without activating the myogenic program. We show that *Myf5* mRNA, together with microRNA-31, which regulates its translation, is sequestered in mRNP granules present in the quiescent satellite cell. In activated satellite cells, mRNP granules are dissociated, relative levels of miR-31 are reduced, and Myf5 protein accumulates, which initially requires translation, but not transcription. Conditions that promote the continued presence of mRNP granules delay the onset of myogenesis. Manipulation of miR-31 levels affects satellite cell differentiation ex vivo and muscle regeneration in vivo. We therefore propose a model in which posttranscriptional mechanisms hold quiescent stem cells poised to enter a tissue-specific differentiation program.

INTRODUCTION

Adult tissue-specific stem cells that contribute to regeneration in response to tissue damage are primed to enter a differentiation program, while remaining quiescent. Examination of the satellite cells of skeletal muscle gives new insight into how these two characteristics may be reconciled. Satellite cells lie under the basal lamina of the muscle fiber unless activated during postnatal growth or after injury, when they leave their niche, replicate, and then differentiate to form new fibers or replenish the satellite cell pool (Buckingham and Montarras, 2008). During development, skeletal muscle progenitor cells express *Pax3* and/or *Pax7*, which are required for the maintenance of this proliferating reserve cell population, as well as for the activation of the myogenic determination genes *Myf5* and *MyoD*, with consequent rapid muscle differentiation (Relaix et al., 2005). Satellite cells also express *Pax7* (Seale et al., 2000) or both *Pax7* and *Pax3* in many muscles (Relaix et al., 2006); however, unlike their embryonic counterparts, more than 95% have already activated the *Myf5* gene in the course of their history (Kuang et al., 2007), indicating that they had entered the myogenic program. Furthermore, the majority of quiescent satellite cells maintain *Myf5* transcription (Beauchamp et al., 2000; Pallafacchina et al., 2010). Here, we examine the posttranscriptional mechanisms that function to repress the translation of *Myf5* mRNA, thereby holding quiescent satellite cells poised to enter the myogenic program.

RESULTS

miR-31 Targets *Myf5* mRNA, Preventing Myf5 Protein Accumulation in the Quiescent Satellite Cell

The majority of quiescent satellite cells transcribe the *Myf5* gene (Beauchamp et al., 2000) and are identifiable by the expression of β-galactosidase from the $Myf5^{nlacZ}$ allele (Figure 1A). Quiescent satellite cells on freshly isolated fibers from wild-type extensor digitorum longus (EDL) muscle are characterized by Pax7 expression, whereas under similar conditions, Myf5 protein is not detectable (Figure 1B). After 24 hr of culture, satellite cells are activated and express the myogenic factors Myf5 and MyoD, as well as Pax7 (Figures 1C and 1D). In the *nlacZ* reporter introduced into the $Myf5^{nlacZ}$ allele, the 3′ UTR of *Myf5* has been replaced by that of SV40. Since microRNAs repress mRNA translation through the 3′ UTR, we investigated posttranscriptional regulation of *Myf5* mRNA by microRNA in the quiescent satellite cell.

We had previously shown that a conserved sequence in the 3′ UTR of *Myf5* mRNA is a target of miR-31 (Daubas et al., 2009). Therefore, we first examined levels of Myf5 protein, *Myf5* mRNA, and miR-31 in satellite cells (Figure 1E) isolated by flow cytometry from adult skeletal muscle of $Pax3^{GFP/+}$ mice (Montarras et al., 2005), which are mainly quiescent, with cells isolated from 1 week postnatal muscle (P7) or adult dystrophic muscle of $Pax3^{GFP/+}$; *mdx:mdx* mice, which are about 80% or 30% activated, respectively (Pallafacchina et al., 2010). Myf5 protein accumulates in activated compared to quiescent satellite cells. Relative *Myf5* transcript levels do not change, whereas miR-31 is higher in quiescent satellite cells. We confirmed the presence of miR-31 by in situ hybridization (ISH) in quiescent satellite cells (Figures 1F and 1G), identified by their expression of Pax7 and their position under the basal lamina (Figures 1H

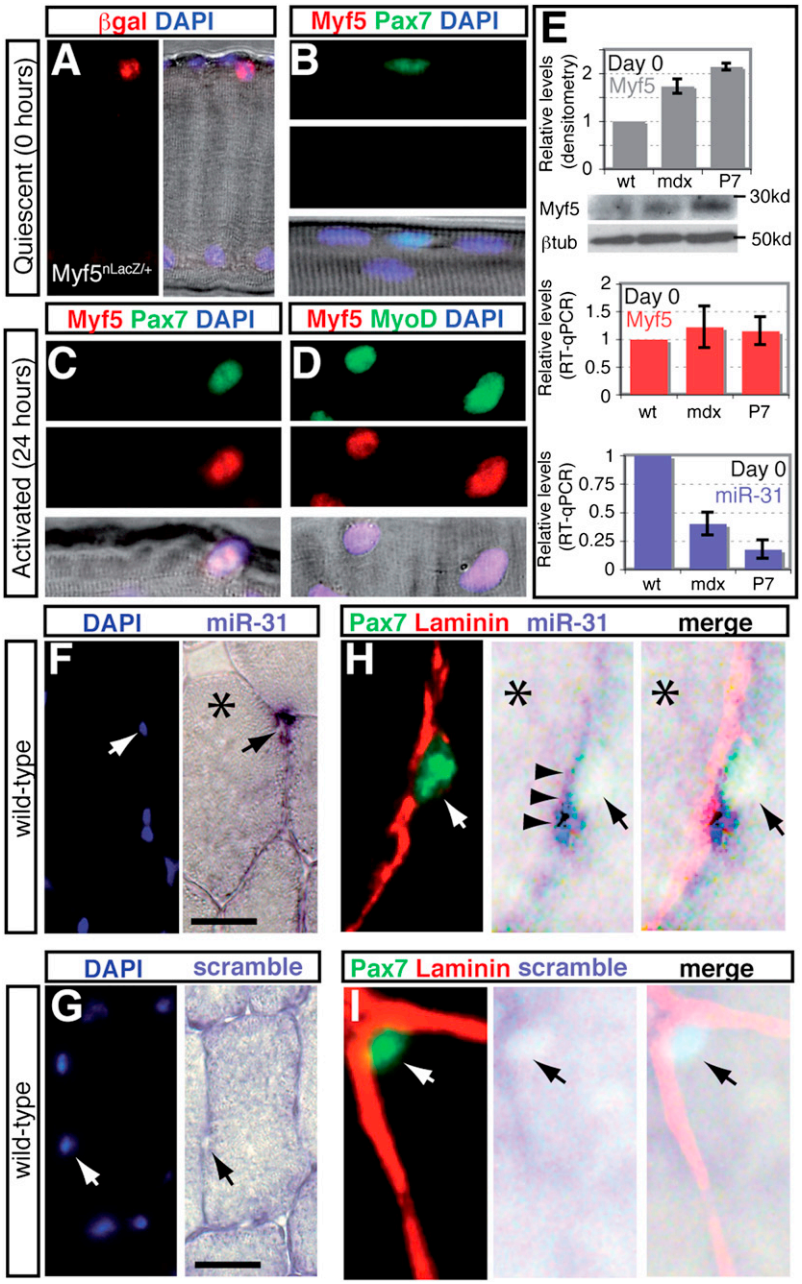

Figure 1. Myf5 and miR-31 Expression in Quiescent and Activated Satellite Cells

(A) Immunostaining with antibodies against β-galactosidase (β-gal; red) on a freshly isolated (0 hr) EDL muscle fiber from a *Myf5*$^{nlacZ/+}$ mouse. Right panel shows merged image with DAPI.

(B) Immunostaining with Pax7 (green, top) and Myf5 (red, middle) antibodies on a freshly isolated (0 hr) wild-type EDL fiber.

(C and D) Immunostaining on EDL fibers, after 24 hr of culture, with Pax7 (green, top left), Myf5 (red, middle), and MyoD (green, top right) antibodies. Merged images with DAPI are shown in the bottom panels of (B), (C), and (D).

(E) Western blot analysis of Myf5 protein levels (normalized to β-tubulin, β-tub) (top) with quantitative PCR analysis of *Myf5* transcripts (normalized to *Actb* transcripts) (middle) and miR-31 levels (normalized to U6 snRNA) (bottom) in satellite cells directly isolated (day 0) from adult *Pax3*$^{GFP/+}$ (wt), adult *Pax3*$^{GFP/+}$; *mdx:mdx* (*mdx*), or postnatal day 7 (P7) *Pax3*$^{GFP/+}$ mice. Error bars represent standard error of the mean (SEM) of three replicate experiments.

(F–I) Sections of adult Tibialis anterior (TA) muscle showing miR-31 (F; purple) detected by ISH in a satellite cell (arrows) marked by DAPI or by ISH with a scrambled oligonucleotide probe (G; scramble, purple). Scale bars represent 20 μm. Combined detection of proteins by immunostaining of TA sections with antibodies to Pax7 and laminin (left), with miRNA ISH (middle) for miR-31 (H; purple, arrowheads), or a scrambled probe (I). Merged images are shown in the right panels. Satellite cells, marked by a Pax7-positive nucleus (green), are indicated by arrows. Asterisks (*) in (F) and (H) mark adjacent fibers, negative for miR-31.

and 1I). In contrast, muscle fibers (Figures 1F and 1H) and other cell types (data not shown) present in the muscle tissue are negative.

miR-31 Is Sequestered with *Myf5* Transcripts in Cytoplasmic mRNP Granules in the Quiescent Satellite Cell

Quiescent cells have a higher level of transcripts for many factors found in mRNP granules (see Table S1 available online; Pallafacchina et al., 2010), which share components with P-bodies and stress granules and have been described as sites of mRNA storage (Buchan and Parker, 2009). Given the evidence for the presence of miRNAs (Liu et al., 2005) and for reversible miRNA repression of mRNA in such granules (Bhattacharyya et al., 2006), we investigated whether *Myf5* mRNA is sequestered with miR-31 during quiescence.

We used antibodies on single fiber preparations to detect components of mRNP granules (Kedersha and Anderson, 2007), for which the transcripts are upregulated in quiescent satellite cells. These include Tia1, a general repressor of translation (Buchan and Parker, 2009), and p54/RCK (Ddx6), which has, in addition, been identified as a direct binding partner of Argonaute2 that functions in miRNA-mediated translational repression (Chu and Rana, 2006). The *Saccharomyces cerevisiae* homolog of p54/RCK, Dhh1, is a component of large mRNA storage granules in quiescent or stationary phase yeast. When growth resumes, mRNA is released from these granules and re-enters translation (Brengues et al., 2005). Both Tia1 and p54/RCK are found in punctate foci corresponding to mRNP granules in the cytoplasm of quiescent satellite cells (Figures 2A and 2B), whereas foci are absent from activated satellite cells after fiber culture (Figures 2D and 2E). The mRNP granules observed are distinct from stress granules, characterized by the presence of HuR (Kedersha and Anderson, 2007; Buchan and Parker, 2009), which remains nuclear in quiescent and activated satellite cells after 24 hr of culture (Figures 2C and 2F). GW182, which interacts directly

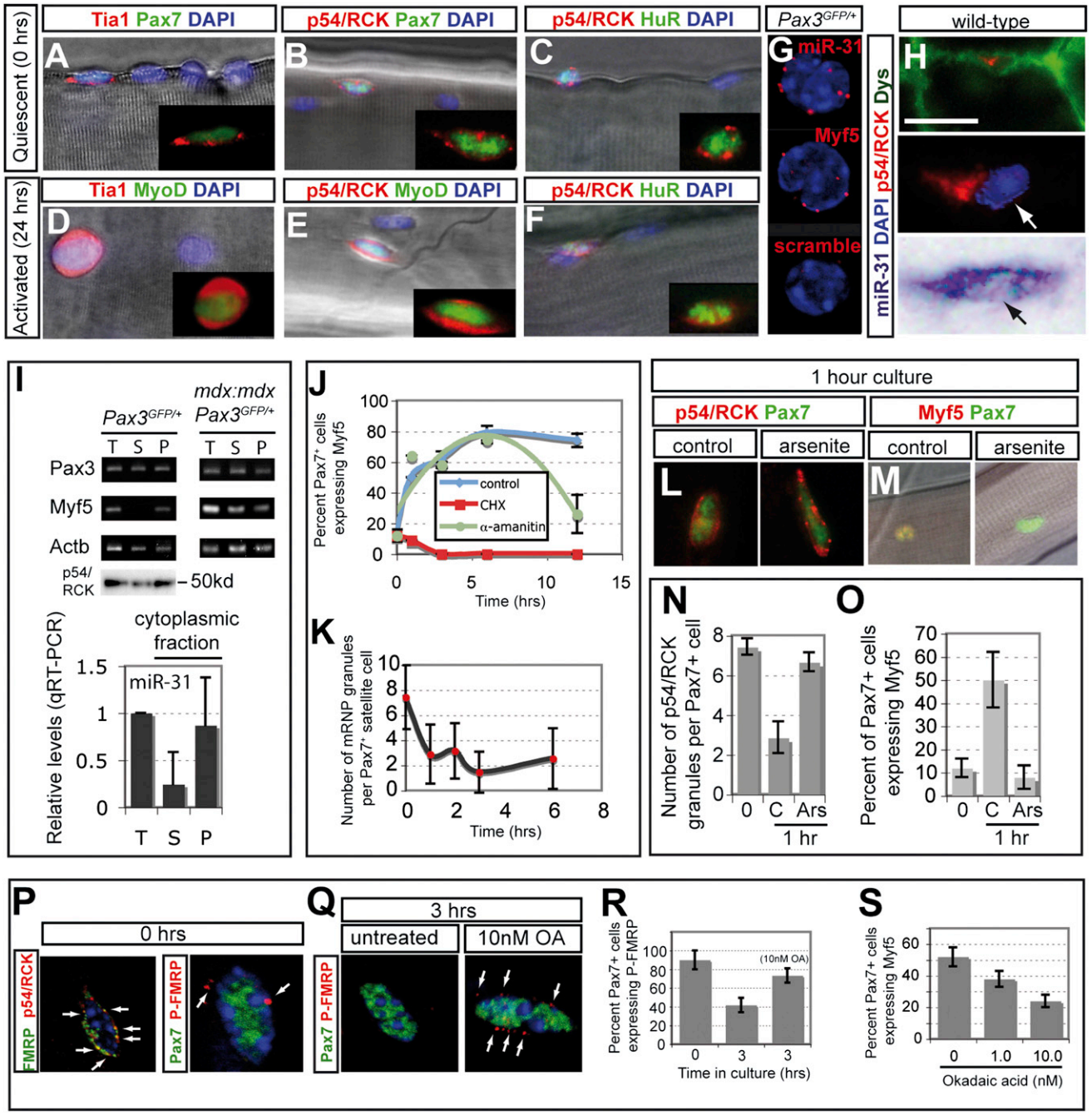

Figure 2. mRNP Granules Contain *Myf5* Transcripts and miR-31 in the Quiescent Satellite Cell

(A–C) Immunostaining with Pax7, Tia1, p54/RCK, and HuR antibodies on EDL fibers shows Tia1 (red) (A) and p54/RCK (red) (B) localization to cytoplasmic granules in a quiescent satellite cell marked by Pax7 (green). HuR (green) remains in the nucleus of a quiescent satellite cell identified by p54/RCK foci (C).

(D–F) After 24 hr of culture, Tia1 (red) (D) and p54/RCK (red) (E) show diffuse cytoplasmic localization in activated satellite cells marked by MyoD-positive (green) nuclei. p54/RCK and HuR show diffuse cytoplasmic (red) and nuclear (green) staining, respectively (F). Insets in (A)–(F) show enlargements of the satellite cells without DAPI staining of the nucleus.

(G) Fluorescent in situ hybridization (FISH) for miR-31 (top), *Myf5* transcripts (middle), and a scrambled-miR probe (scramble, bottom) on quiescent satellite cells freshly isolated from *Pax3*$^{GFP/+}$ adult muscle.

(H) Immunofluorescent labeling on sections of adult TA muscle; p54/RCK (red) shows the presence of cytoplasmic mRNP granules in a satellite cell, outlined by characteristic dystrophin labeling (green) of the contour of the muscle fiber (top). The same satellite cell is shown enlarged, labeled for p54/RCK and DAPI (middle), followed by ISH for miR-31 (purple, bottom). Arrows denote the nucleus.

(I) Cytoplasmic fractions from freshly isolated in vivo quiescent satellite cells from adult *Pax3*$^{GFP/+}$ muscle (left) and in vivo activated satellite cells from *Pax3*$^{GFP/+}$; *mdx:mdx* muscle (right) were analyzed by RT-PCR for *Pax3*, *Myf5*, and *Actb* transcripts (top) or by qRT-PCR for miR-31, normalized to U6 snRNA (bottom). Error bars represent SEM of three replicate experiments. T, total cell fraction; S, soluble cytoplasmic fraction; P, pelletable cytoplasmic fraction containing mRNP

with Argonaute proteins and is required for miRNA-mediated gene silencing in animal cells (Eulalio et al., 2009), is present in foci in the quiescent satellite cell, whereas it is diffuse in the cytoplasm of the activated satellite cell (Figure S1A). We used ISH to examine the localization of miR-31 and *Myf5* transcripts, which we show are present in punctate cytoplasmic foci (Figure 2G; Figure S1B), where they colocalize with p54/RCK (Figure 2H; Figure S1C).

To further investigate accumulation of miR-31 and *Myf5* transcripts in mRNP storage granules, we fractionated by centrifugation cytoplasmic extracts (Bhattacharyya et al., 2006) of quiescent (*Pax3*$^{GFP/+}$) and activated (*Pax3*$^{GFP/+}$; *mdx:mdx*) satellite cells. *Pax3* transcripts are abundant in the soluble fraction of quiescent and activated satellite cells. *Myf5* transcripts and miR-31 are accumulated in the pelletable mRNP fraction of quiescent satellite cells, whereas *Myf5* transcripts are present in the soluble fraction of activated satellite cells (Figure 2I). In keeping with this, *Myf5* transcripts and miR-31 are coimmunoprecipitated by anti-p54/RCK antibodies from whole-cell lysates of quiescent satellite cells. In lysates of activated satellite cells, p54/RCK remains associated with residual miR-31, but not with *Myf5* transcripts (Figures S1D and S1E). Polysome gradients show *Myf5* transcripts and miR-31 in the prepolysome light fraction in quiescent satellite cells, whereas *Myf5* transcripts are highly enriched in the polysome fraction of activated satellite cell lysates (Figures S1F–S1H).

Satellite cells on single EDL fibers rapidly upregulate Myf5 protein, even in the presence of α-amanitin, which blocks transcription and degrades the Rbp1 subunit of RNA polymerase II (Figure S2C; Nguyen et al., 1996), but not in the presence of cycloheximide, which blocks translation (Figure 2J). The timing of Myf5 upregulation corresponds to that of the disassembly of mRNP granules (Figure 2K), which takes place very rapidly when satellite cells are activated in culture. When 1.0 mM sodium arsenite is added to the culture medium at time 0, p54/RCK-containing mRNP granules, which sequester *Myf5* mRNA, continue to be observed (Figures 2L and 2N; Figure S2), and Myf5 protein does not accumulate (Figures 2M and 2O) in satellite cells. Formation of new stress granules under these conditions is precluded by the absence of HuR, a component of this type of cytoplasmic granule, (Kedersha and Anderson, 2007; Buchan and Parker, 2009), which remains nuclear (Figure S2B).

We investigated the mechanism by which *Myf5* transcripts are rapidly released from miR-31 repression upon satellite cell activation. HuR is essential for the release of transcripts from microRNA activity in cells subjected to stress (Bhattacharyya et al., 2006), but it remains nuclear in activated satellite cells (Figure 2F). We therefore examined FMRP, a component of some types of mRNP granules (Buchan and Parker, 2009); FMRP phophorylation promotes microRNA activity in neurons (Muddashetty et al., 2011). We also find phospho-FMRP in mRNP granules of quiescent satellite cells (Figure 2P), whereas it is not detectable on activation (Figure 2Q). Inhibition of protein phosphatase 2A-dependent dephosphorylation of FMRP by okadaic acid, which prevents mRNA dissociation from Ago2 in neurons (Muddashetty et al., 2011), also prevents the accumulation of Myf5 protein in satellite cells on cultured fibers (Figures 2R and 2S). Levels of miR-31 are unaffected (Figure S2D).

Satellite Cell Behavior Is Modified by miR-31 Regulation of Myf5 Expression

We next examined the effect of sustained miR-31 expression on the myogenic program. Satellite cells were isolated from muscles of adult *Pax3*$^{GFP/+}$ mice and cultured for 3 days, when many cells express Myf5 and some are positive for the myogenic differentiation factor Myogenin (Figure 3A). Transfection of satellite cells with miR-31 precursors (Figure S3A) reduced Myf5 expression, resulting in a delay in the onset of differentiation indicated by the absence of Myogenin (Figures 3B and 3E). After 4 days in culture, most satellite cells normally express Myogenin and muscle TroponinT with formation of multinucleated myotubes (Figure 3C); however, this progression is delayed after transfection of miR-31 precursors (Figures 3D and 3E). Reduced Myf5, Myogenin, and TroponinT in satellite cell cultures transfected with miR-31 precursor molecules was confirmed by western blotting (Figure S3B). Transfection of satellite cells with miR-31 inhibitors had no detectable effect (data not shown), consistent with miR-31 downregulation

granules. Increased concentration of mRNP granules in the pelletable compared to soluble cytoplasmic fraction from quiescent satellite cells is shown by western blotting with antibodies against p54/RCK (middle).

(J) Quantitation of coexpression of Pax7 and Myf5, monitored by immunostaining, on satellite cells of freshly isolated EDL fibers cultured in the presence of 10 μg/ml α-amanitin (green) or 100 μg/ml cycloheximide (CHX, red). Error bars represent SEM of three independent single fiber cultures. See also Table S1 and Figure S1.

(K) Quantitation of the number of mRNP granules upon activation of satellite cells (marked by Pax7) on cultured EDL fibers over time, visualized by immunostaining with antibodies against p54/RCK. Error bars represent SEM with n > 50 at each time point.

(L and M) Immunostaining with Pax7 (green), p54/RCK (red), and Myf5 (red) antibodies on satellite cells after 1 hr of EDL fiber culture, in the absence (control) or presence of 1 mM sodium arsenite.

(N and O) Quantification of the number of granules per Pax7-positive satellite cell on isolated EDL fibers (N) and percentage of Pax7-positive satellite cells that show immunofluorescence for Myf5 in these satellite cells (O). 0, freshly isolated fibers; C, control fibers after 1 hr culture; Ars, fibers cultured for 1 hr in the presence of 1 mM sodium arsenite. Error bars represent SEM.

(P) Immunostaining with Pax7, p54/RCK, FMRP, and phosphospecific FMRP (P-FMRP) antibodies on freshly isolated (0 hr) EDL fibers. Arrows show FMRP localization to p54/RCK (red) containing granules and P-FMRP (red) localization to granules in quiescent satellite cells where the nucleus is marked by Pax7 (green).

(Q) Immunostaining with P-FMRP (red) and Pax7 (green) antibodies after 3 hr of EDL fiber culture in the absence (control) or presence of 10 nM Okadaic acid (OA). Arrows point to P-FMRP in granules.

(R and S) Percentage of Pax7-positive satellite cells that show immunofluorescence for P-FMRP (R) and Myf5 (S) in satellite cells on 0, freshly isolated fibers, or 3, fibers after 3 hr culture in the absence or presence of 1 or 10 nM OA, as indicated. Error bars represent SEM.

See also Figure S2.

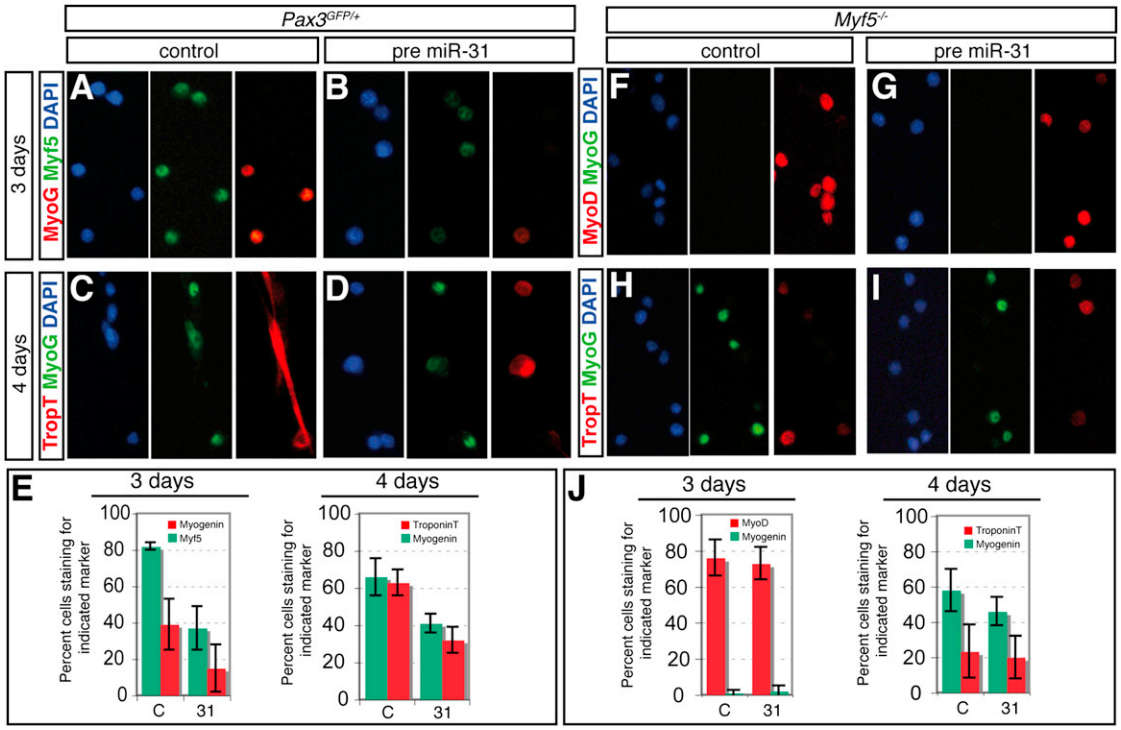

Figure 3. Differentiation of Activated Satellite Cells Is Modulated by miR-31 Regulation of Myf5 Protein Levels

(A and B) Detection of Myf5 (green) and Myogenin (MyoG) (red) by immunocytochemistry with the corresponding antibodies after satellite cells were transfected with control (A) or pre-miR-31 (B) precursor oligonucleotides and cultured for 3 days.

(C and D) After 4 days in culture, immunocytochemistry with antibodies against MyoG (green) and TroponinT (TropT, red) on control or pre-miR-31-transfected satellite cells.

(E) The percentage of satellite cells expressing Myf5, Myogenin, and TroponinT, monitored by immunocytochemistry, after 3 and 4 days in culture, of control-transfected (C) and pre-miR-31-transfected (31) satellite cells isolated from adult *Pax3*$^{GFP/+}$ mice. Error bars represent SEM of three independent cultures with $p < 0.001$ using paired Student's t test. See also Figure S3.

(F–I) Detection of MyoG (green) with MyoD (red) (F and G) or TropT (red) (H and I) by immunocytochemistry with the corresponding antibodies after satellite cells isolated from adult *Myf5*$^{-/-}$ mice were transfected with control (F and H) or pre-miR-31 (G and I) precursor oligonucleotides and cultured for 3 (F and G) or 4 (H and I) days.

(J) Percentage of satellite cells, isolated from adult *Myf5*$^{-/-}$ mice, expressing MyoD, Myogenin, and TroponinT, monitored by immunocytochemistry, after 3 and 4 days in culture, after transfection with pre-miR-31 (31) and control (C) oligonucleotides. Error bars represent SEM of three independent cultures.

in cultured satellite cells. When miR-31 precursors were transfected into satellite cells isolated from *Myf5*$^{-/-}$ mice, no delay in differentiation was observed (Figures 3F–3J), demonstrating that *Myf5* transcripts are the primary target of miR-31 in wild-type satellite cells.

In dystrophic *mdx* muscle, miR-31 is abnormally upregulated (Cacchiarelli et al., 2011). We show that this is also the case in satellite cells and that inhibition of miR-31 results in increased Myf5 protein levels and improved differentiation (Figures S4A–S4E).

We next examined miR-31 function in satellite cells in vivo by antagomiR-mediated inhibition (Krützfeldt et al., 2005). AntagomiRs against miR-31 (antagomiR-31) accumulate in satellite cells after intravenous injection (Figures S3C and S3D) and result in increased numbers of Pax7-positive satellite cells (Figures 4A and 4E), Myf5 protein accumulation (Figures 4B and 4F), loss of mRNP granules (Figures 4C and 4G), and cell cycle re-entry as evidenced by Ki67 labeling of MyoD-positive satellite cells (Figure 4D). More myonuclei are present (Figure 4H), and muscle fibers are larger (Figure 4I).

In regenerating muscle after injury, satellite cells are activated and form new fibers, with reconstitution of the satellite cell pool. Ten days after cardiotoxin injury of the Tibialis anterior (TA) muscle, mice treated with antagomiR-31 had increased levels of Myf5-positive progenitors compared to controls in areas that did not stain positive for myosin heavy chain, which marks differentiated fibers (Figure 4J). In the presence of antagomiR-31, there were increased numbers of small, immature fibers marked by embryonic myosin heavy chain (embMHC) (Figures 4K and 4L). The expansion of a pool of myogenic progenitor cells probably accounts for the increase in myofiber size seen later, at 21 days after cardiotoxin injection (Figures 4M and 4N). Efficient inhibition of miR-31 levels by antagomiR-31 in TA muscle was shown by qRT-PCR (Figures S3E and S3F). Similar results to those in cardiotoxin-injured muscle were seen after antagomiR-31 treatment in *mdx* muscle (Figures S4F–S4K).

We also examined the effect of injury on the presence of mRNP granules. On transverse sections of uninjured TA muscle, p54/RCK-labeled foci are observed in all satellite cells

(Figure 4G). The number and size of foci were decreased 21 days after cardiotoxin injury, with only 65% of satellite cells, marked by Pax7, containing detectable foci (Figures 4O and 4P). AntagomiR-31 treatment further decreased the number of Pax7-positive satellite cells with detectable foci to 45% (Figure 4P), suggesting that 21 days after injury, more satellite cells were still activated and contributing to fiber growth. This is consistent with the increase in fiber size in these muscles and the activating effect of antagomiR-31 on satellite cells of uninjured muscle.

DISCUSSION

We conclude that in quiescent satellite cells, *Myf5* mRNA is sequestered in mRNP granules, where the presence of miR-31 ensures silencing. On activation, mRNP granules dissociate, releasing *Myf5* transcripts, leading to rapid translation and accumulation of the Myf5 protein, which promotes myogenesis. This mechanism is consistent with reports that P-bodies also function in miRNA-mediated translational repression (Liu et al., 2005), as well as mRNA storage, in mammalian cells (Bhattacharyya et al., 2006) and in yeast (Brengues et al., 2005). In the latter, the transition from stationary phase to growth, reminiscent of the transition from quiescent to activated satellite cells, is accompanied by breakdown of the mRNP granules and rapid mRNA translation. When muscle is injured, signaling pathways are activated. We propose that this leads to rapid dephosphorylation of FMRP, with consequent *Myf5* transcript release for translation. Other effects on mRNP protein modifications probably contribute to their dissociation.

We show that transcripts of the endogenous *Myf5* gene are present and that their level does not increase on activation relative to a β*−actin* control sequence. This quantitative comparison is complicated by the low transcriptional activity in quiescent satellite cells. However, whereas many sequences show striking upregulation on activation (Pallafacchina et al., 2010), this is not the case for *Myf5* mRNA. Furthermore, inhibition of transcription does not prevent the initial rapid accumulation of Myf5 protein on activation, consistent with posttranscriptional regulation. In contrast to *Myf5* transcripts, miR-31 levels, measured relative to U6 RNA, are lower in activated satellite cells. The relative level of miR-31 to its target *Myf5* mRNA therefore falls. The inhibitory effect of miR-31 is further accentuated by concentration with *Myf5* mRNA in mRNP granules in the quiescent cell. On activation, *Myf5* mRNA is released from miR-31 repression, mediated by FMRP dephosphorylation, and enters polysomes. Abnormally high levels of miR-31 that we observe in activated satellite cells, as well as muscle fibers (Cacchiarelli et al., 2011) of dystrophic muscle, probably contribute to the pathology. This should be therapeutically accessible to antagomiR treatment (Williams et al., 2009).

The myogenic determination factor, MyoD, is also present in activated satellite cells (Buckingham and Montarras, 2008) and will compensate for downregulation of Myf5. However, we observe that myogenesis is delayed when Myf5 accumulation is compromised. This is in keeping with observations on *Myf5* mutant mice in which a delay in differentiation was reported, linked to a proliferative defect (Montarras et al., 2000; Gayraud-Morel et al., 2007; Ustanina et al., 2007). Myf5 promotion of proliferation would account for the increase in activated satellite cells both in uninjured and injured muscle treated with an antagomiR to miR-31. The later increase in muscle fiber size that results from Myf5 overexpression is also consistent with the converse reduction in muscle fiber size reported in the absence of Myf5 (Ustanina et al., 2007).

In conclusion, manipulations that affect Myf5 protein accumulation have repercussions on myogenesis and muscle regeneration. Interference with miR-31 or mRNP granules compromises the normal progression of satellite cell activation by maintaining the brakes that function through these mechanisms to prevent Myf5 accumulation in the quiescent satellite cell. We suggest that similar mechanisms may apply to other adult stem cells, which have acquired tissue specificity and are poised for regeneration while remaining quiescent.

EXPERIMENTAL PROCEDURES

Cell and Single Fiber Culture

Satellite cells were isolated from the abdominal muscle and diaphragm of 1-week-old (P7), 5- to 6-week-old (adult) *Pax3*$^{GFP/+}$, or 5- to 6-week-old *Pax3*$^{GFP/+}$; *mdx:mdx* mice, sorted by flow cytometry (Montarras et al., 2005) and cultured for the times indicated. Alternatively, satellite cells were sorted from the same muscles of adult *Myf5*$^{-/-}$ mice (kindly provided by T. Braun; Ustanina et al., 2007) using antibodies against CD34 as previously described (Montarras et al., 2005). Sorted cells were reverse transfected with either microRNA precursor or inhibitor oligonucleotides (Ambion) as described previously (Crist et al., 2009). Increased miR-31 levels were confirmed by qRT-PCR (Figure S3) as described below. Single fibers were isolated from the EDL muscle of adult mice and cultured. Where indicated, cultures were supplemented with 10 μg/ml α-amanitin (Sigma), 100 μg/ml cycloheximide (Sigma), 1.0 mM sodium arsenite (Sigma), or 1.0–10.0 nM okadaic acid (Sigma).

In Situ Hybridization

Endogenous miR-31 and *Myf5* transcripts were detected in formaldehyde and 1-ethyl-3-(3-dimethylaminopropyl) carbodiimide (EDC, Fluka), as described (Pena et al., 2009), on fixed sections or on satellite cells isolated from *Pax3*$^{GFP/+}$ mice deposited on a slide by cytospin. Probes were 5′ and 3′ dual DIG-conjugated locked nucleic acid (LNA) probe against miR-31 (Exiqon), a scramble-miR control probe (Exiqon), and a DIG-labeled probe against *Myf5* (Daubas et al., 2009). Prehybridization and hybridization was at 60°C for miR-31, 58°C for scramble-miR, and 68°C for *Myf5* transcripts.

Cell Fractionation, RNA, and Protein Analysis

Digitonin permeabilization, followed first by a centrifugation to separate cytoplasmic contents from intact nuclei, followed by centrifugation at 14,000 rpm for 15 min of the cytoplasmic components to pellet mRNP granules, was performed as described (Bhattacharyya et al., 2006). The resulting supernatant and pellet fractions were analyzed for the presence of p54/RCK by western blotting as well as for mRNAs and miR-31 by RT-PCR as described below. Immunoprecipitation of RNA-protein complexes (Peritz et al., 2006) and polyribosome gradient fractionations (Bhattacharyya et al., 2006) were performed as described. RNA was harvested from cells, fractionated cells, or muscle tissues by using TRIzol reagent (Invitrogen) and treated with DNase (Roche). Detection of miR-31 by quantitative RT-PCR was performed using the miRCURY LNA Universal RT-PCR system (Exiqon) according to the manufacturer's instructions. Amplification of U6 snRNA was used to normalize the data. For detection of mRNAs, total RNA was reverse transcribed with a random primer (Exiqon) by using SuperScript II reverse transcriptase (Invitrogen). RT-PCR primers were forward 5′-CTGTCTGGTCCCGAAAGAAC-3′ and reverse 5′-AAGCAATCCAAGCTGGACAC-3′ *Myf5*; forward 5′-CAACC AGGAGGAGCGCGATCTCCG′3′ and reverse 5′-AGGCGCTGTGGGAGTTG CATTCACT-3′ *Myogenin*; forward 5′- AAACATCCCCCAAAGTTCTAC-3′ and reverse 5′-GAGGGACTTCCTGTAACCACT-3′ *Actb*. qRT-PCRs were performed with SYBR Green PCR Master Mix (Applied Biosystems). For protein analysis, cell lysates were prepared as described (Crist et al., 2009) and

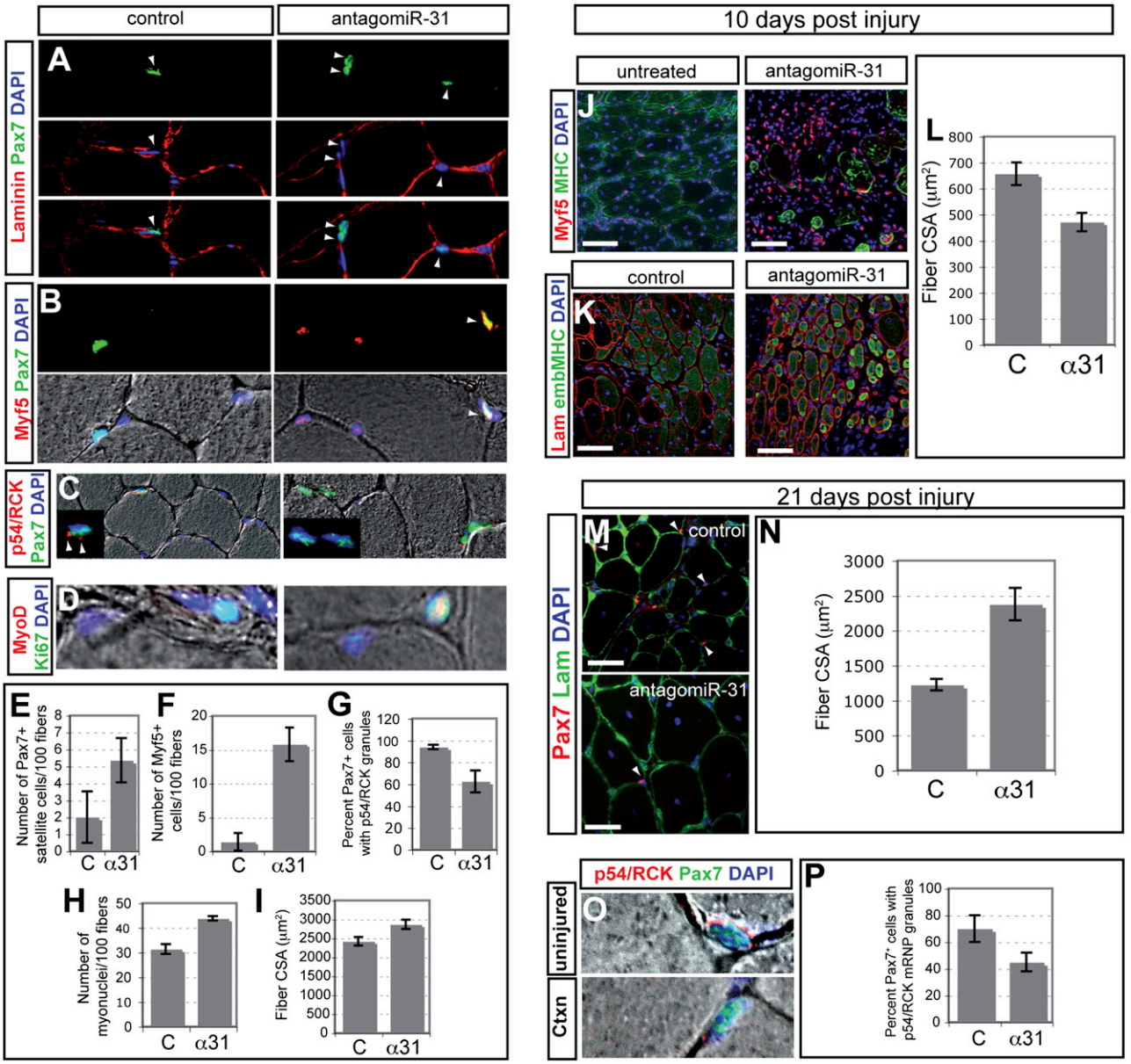

Figure 4. Satellite Cell Activity and Skeletal Muscle Regeneration Is Modulated by miR-31 Regulation of Myf5

(A–I) Uninjured TA muscle after antagomiR-31 treatment.

(A) Immunostaining of sections with antibodies against Pax7 (top, green) and laminin (middle, red), with DAPI staining of nuclei, in mice treated with antagomiRs against miR-31 (antagomiR-31) or a control antagomiR. Merged images are shown in the bottom panels. Arrowheads point to satellite cells.

(B) Immunostaining of sections with antibodies against Pax7 (green) and Myf5 (red) in mice treated with antagomiR-31 or a control antagomiR. Merged images, with DAPI staining, are shown in the bottom panels. Colocalization of Myf5 with Pax7 (yellow) in a satellite cell of antagomiR-31-treated mice is indicated (arrowheads).

(C) Immunostaining of sections with antibodies against Pax7 (green) and p54/RCK (red) of antagomiR-31, compared to control antagomiR-treated animals. Insets show enlargement of satellite cells with DAPI staining of the nucleus.

(D) Immunostaining of sections with antibodies against MyoD (red) and Ki67 (green), with DAPI staining of the nuclei, of antagomiR-31, compared to control antagomiR-treated mice.

(E and F) Quantification of the number of satellite cells expressing Pax7 (E) and Myf5 (F), per 100 fibers, on such transverse sections of TA muscle from mice treated with control antagomiR (C) or antagomiR-31 (α31). Error bars represent SEM.

(G) Percentage of Pax7-positive satellite cells with cytoplasmic mRNP granules labeled by p54/RCK on transverse sections of TA muscles from mice treated with control antagomiR (C) or antagomiR-31 (α31). Error bars represent SEM.

(H) Quantification of the number of myonuclei per 100 fibers on sections of TA muscle from mice treated with control antagomiR (C) or antagomiR-31 (α31). Error bars represent SEM.

(I) The mean TA muscle fiber cross-section area (CSA) from mice treated with control antagomiR (C) or antagomiR-31 (α31). Error bars represent 95% confidence interval surrounding the mean with $p < 0.001$ using paired Student's t test.

western blots were performed using polyclonal anti-Myf5 (Santa Cruz), monoclonal anti-Myogenin (Dako), anti-TroponinT (Sigma), and anti-β-tubulin (Millipore) antibodies. Blots were exposed to Hyperfilm ECL (GE Healthcare) and densitometry was performed with ImageJ software (NIH). Data were normalized to the expression of β-tubulin.

Immunofluorescence

Formalin-fixed, cultured *Pax3*$^{GFP/+}$ satellite cells were permeabilized and blocked as described previously (Crist et al., 2009). For the detection of mRNP granules, *Pax3*$^{GFP/+}$ cells deposited on a slide by cytospin, single fibers, or frozen transverse sections were permeabilized and blocked as described previously (Kedersha and Anderson, 2007). Primary antibodies used were monoclonal anti-β-galactosidase (a kind gift from J.F. Nicolas), anti-Pax7 (DHSB), anti-MyoD (Dako), anti-TroponinT (Sigma), anti-Dystrophin Dys2 (Dako), anti-GW182 (abcam), anti-HuR (Santa Cruz), anti-embryonic myosin heavy chain G6 (DHSB,) anti-myosin heavy chain MF20 (DHSB), anti-FMRP (DHSB), anti-Ki67 (BD PharMingen), polyclonal anti-Myf5 (Santa Cruz), anti-Myogenin (Santa Cruz), anti-p54/RCK (Bethyl), anti-TIA1/TIAR (Santa Cruz), and anti-phospho-FMRP (abcam).

Muscle Regeneration

Care and handling of animals were in accordance with the regulations of the French Ministry of Agriculture and Fisheries, as practised by the Institut Pasteur animal facility.

On day 1, 8-week-old Swiss mice were anesthetized by intraperitoneal injection of a mixture of Imalgene/Rompun. A 10 μl solution of 10 μM cardiotoxin (Latoxan) was injected into the tibialis anterior (TA) muscle. AntagomiRs (Krützfeldt et al., 2005) were against miR-31 (antagomiR-31; 5′-mC*mA*mGmCmUmAmUmGmCmCmAmGmCmAmUmCmUmU*mG*mC*mC*mC*mU-3′-Chl) and against *Caenorhabditis elegans* miR-67 (control; 5′-mU*mA*mCmUmCmUmUmUmCmUmAmGmGmAmGmGmU*mU*mG*mU*mG-3′-Chl), which has minimal sequence identity to mammalian microRNAs. The m denotes 2′Me-O modifications, asterisk denotes phosphothioate linkers, and the Chl denotes a cholesterol moiety. For flow cytometry, antagomiR-31 was 5′ conjugated to the fluorophore Dy547 (Thermo Scientific). AntagomiRs were delivered by tail vein injection (40 mg/kg) on day 3 and day 7 (10 day analysis) or day 7 and day 14 (21 day analysis) in injury studies or to adult 8-week-old *mdx:mdx* mice on day 1 and day 7 before analysis on day 10. TA and diaphragm muscles were harvested and immediately frozen in isopentane cooled in liquid nitrogen and stored at −80°C, prior to immunofluorescent labeling or measurement of miR-31 levels.

Statistical Analysis

The SEM, 95% confidence intervals and paired Student's t tests, were calculated using Microsoft Excel software, as indicated.

SUPPLEMENTAL INFORMATION

Supplemental Information includes four figures and one table and can be found with this article online at http://dx.doi.org/10.1016/j.stem.2012.03.011.

ACKNOWLEDGMENTS

We are thankful to S. Coqueran, P.H. Commere, M. Livingstone, and F. Lescroart for technical assistance. T. Braun (MPI, Bad Nauheim) generously provided the *Myf5*$^{-/-}$ mouse line. This work was supported by the Institut Pasteur and the CNRS, as well as by grants from the AFM and EU networks EuroSyStem (Health F4-2007, 200720) and OptiStem (Health FP7-2007, 223098), which also supported C.G.C.

Received: August 8, 2011
Revised: December 30, 2011
Accepted: March 19, 2012
Published: July 5, 2012

REFERENCES

Beauchamp, J.R., Heslop, L., Yu, D.S., Tajbakhsh, S., Kelly, R.G., Wernig, A., Buckingham, M.E., Partridge, T.A., and Zammit, P.S. (2000). Expression of CD34 and Myf5 defines the majority of quiescent adult skeletal muscle satellite cells. J. Cell Biol. *151*, 1221–1234.

Bhattacharyya, S.N., Habermacher, R., Martine, U., Closs, E.I., and Filipowicz, W. (2006). Relief of microRNA-mediated translational repression in human cells subjected to stress. Cell *125*, 1111–1124.

Brengues, M., Teixeira, D., and Parker, R. (2005). Movement of eukaryotic mRNAs between polysomes and cytoplasmic processing bodies. Science *310*, 486–489.

Buchan, J.R., and Parker, R. (2009). Eukaryotic stress granules: the ins and outs of translation. Mol. Cell *36*, 932–941.

Buckingham, M., and Montarras, D. (2008). Skeletal muscle stem cells. Curr. Opin. Genet. Dev. *18*, 330–336.

Cacchiarelli, D., Incitti, T., Martone, J., Cesana, M., Cazzella, V., Santini, T., Sthandier, O., and Bozzoni, I. (2011). miR-31 modulates dystrophin expression: new implications for Duchenne muscular dystrophy therapy. EMBO Rep. *12*, 136–141.

Chu, C.Y., and Rana, T.M. (2006). Translation repression in human cells by microRNA-induced gene silencing requires RCK/p54. PLoS Biol. *4*, e210.

Crist, C.G., Montarras, D., Pallafacchina, G., Rocancourt, D., Cumano, A., Conway, S.J., and Buckingham, M. (2009). Muscle stem cell behavior is modified by microRNA-27 regulation of Pax3 expression. Proc. Natl. Acad. Sci. USA *106*, 13383–13387.

Daubas, P., Crist, C.G., Bajard, L., Relaix, F., Pecnard, E., Rocancourt, D., and Buckingham, M. (2009). The regulatory mechanisms that underlie inappropriate transcription of the myogenic determination gene Myf5 in the central nervous system. Dev. Biol. *327*, 71–82.

Eulalio, A., Helms, S., Fritzsch, C., Fauser, M., and Izaurralde, E. (2009). A C-terminal silencing domain in GW182 is essential for miRNA function. RNA *15*, 1067–1077.

(J–P) Injured TA muscle after antagomiR-31 treatment.
(J) Immunostaining of sections with antibodies against Myf5 (red) and myosin heavy chain (MHC, green) 10 days after cardiotoxin injury in untreated (left) or antagomiR-31-treated (right) animals.
(K) Immunostaining of sections with antibodies against embryonic myosin heavy chain (embMHC, green) and laminin (red) 10 days after cardiotoxin injury in control antagomiR (left) or antagomiR-31-treated (right) animals. Scale bars in (J) and (K) represent 20 μm.
(L) The mean CSA of embMHC-positive TA fibers, 10 days after cardiotoxin injury, from mice treated with control antagomiR (C) or antagomiR-31 (α31). Error bars represent 95% confidence interval surrounding the mean with $p < 0.001$ using paired Student's t test.
(M) Immunostaining of sections with antibodies against Pax7 (red) and laminin (Lam, green) 21 days after cardiotoxin injury. The position of satellite cells underneath the basal lamina is marked with white arrowheads. Scale bars represent 20 μm.
(N) The mean CSA of regenerating TA fibers (central nuclei), 21 days after cardiotoxin injury, from mice treated with control antagomiR (C) or antagomiR-31 (α31). Error bars represent 95% confidence interval surrounding the mean with $p < 0.001$ using paired Student's t test.
(O) Immunostaining of sections, focusing on satellite cells, with antibodies against p54/RCK (red) and Pax7 (green), 21 days after cardiotoxin injury (Ctxn) and in a contralateral uninjured muscle. Nuclei in sections (J), (K), (M), and (O) are stained with DAPI (blue).
(P) Percentage of Pax7-positive satellite cells containing cytoplasmic mRNP granules as indicated by immunostaining with antibodies against p54/RCK, 21 days after cardiotoxin injury, in untreated (C) and antagomiR-31-treated (α31) animals. Error bars represent SEM.
See also Figures S3 and S4.

Gayraud-Morel, B., Chrétien, F., Flamant, P., Gomès, D., Zammit, P.S., and Tajbakhsh, S. (2007). A role for the myogenic determination gene Myf5 in adult regenerative myogenesis. Dev. Biol. *312*, 13–28.

Kedersha, N., and Anderson, P. (2007). Mammalian stress granules and processing bodies. Methods Enzymol. *431*, 61–81.

Krützfeldt, J., Rajewsky, N., Braich, R., Rajeev, K.G., Tuschl, T., Manoharan, M., and Stoffel, M. (2005). Silencing of microRNAs in vivo with 'antagomirs'. Nature *438*, 685–689.

Kuang, S., Kuroda, K., Le Grand, F., and Rudnicki, M.A. (2007). Asymmetric self-renewal and commitment of satellite stem cells in muscle. Cell *129*, 999–1010.

Liu, J., Valencia-Sanchez, M.A., Hannon, G.J., and Parker, R. (2005). MicroRNA-dependent localization of targeted mRNAs to mammalian P-bodies. Nat. Cell Biol. *7*, 719–723.

Montarras, D., Lindon, C., Pinset, C., and Domeyne, P. (2000). Cultured myf5 null and myoD null muscle precursor cells display distinct growth defects. Biol. Cell *92*, 565–572.

Montarras, D., Morgan, J., Collins, C., Relaix, F., Zaffran, S., Cumano, A., Partridge, T., and Buckingham, M. (2005). Direct isolation of satellite cells for skeletal muscle regeneration. Science *309*, 2064–2067.

Muddashetty, R.S., Nalavadi, V.C., Gross, C., Yao, X., Xing, L., Laur, O., Warren, S.T., and Bassell, G.J. (2011). Reversible inhibition of PSD-95 mRNA translation by miR-125a, FMRP phosphorylation, and mGluR signaling. Mol. Cell *42*, 673–688.

Nguyen, V.T., Giannoni, F., Dubois, M.F., Seo, S.J., Vigneron, M., Kédinger, C., and Bensaude, O. (1996). In vivo degradation of RNA polymerase II largest subunit triggered by alpha-amanitin. Nucleic Acids Res. *24*, 2924–2929.

Pallafacchina, G., François, S., Regnault, B., Czarny, B., Dive, V., Cumano, A., Montarras, D., and Buckingham, M. (2010). An adult tissue-specific stem cell in its niche: a gene profiling analysis of in vivo quiescent and activated muscle satellite cells. Stem Cell Res. *4*, 77–91.

Pena, J.T., Sohn-Lee, C., Rouhanifard, S.H., Ludwig, J., Hafner, M., Mihailovic, A., Lim, C., Holoch, D., Berninger, P., Zavolan, M., and Tuschl, T. (2009). miRNA in situ hybridization in formaldehyde and EDC-fixed tissues. Nat. Methods *6*, 139–141.

Peritz, T., Zeng, F., Kannanayakal, T.J., Kilk, K., Eiríksdóttir, E., Langel, U., and Eberwine, J. (2006). Immunoprecipitation of mRNA-protein complexes. Nat. Protoc. *1*, 577–580.

Relaix, F., Rocancourt, D., Mansouri, A., and Buckingham, M. (2005). A Pax3/Pax7-dependent population of skeletal muscle progenitor cells. Nature *435*, 948–953.

Relaix, F., Montarras, D., Zaffran, S., Gayraud-Morel, B., Rocancourt, D., Tajbakhsh, S., Mansouri, A., Cumano, A., and Buckingham, M. (2006). Pax3 and Pax7 have distinct and overlapping functions in adult muscle progenitor cells. J. Cell Biol. *172*, 91–102.

Seale, P., Sabourin, L.A., Girgis-Gabardo, A., Mansouri, A., Gruss, P., and Rudnicki, M.A. (2000). Pax7 is required for the specification of myogenic satellite cells. Cell *102*, 777–786.

Ustanina, S., Carvajal, J., Rigby, P., and Braun, T. (2007). The myogenic factor Myf5 supports efficient skeletal muscle regeneration by enabling transient myoblast amplification. Stem Cells *25*, 2006–2016.

Williams, A.H., Liu, N., van Rooij, E., and Olson, E.N. (2009). MicroRNA control of muscle development and disease. Curr. Opin. Cell Biol. *21*, 461–469.